

Measuring Global Galaxy Metallicities Using Emission Line Equivalent Widths

Henry A. Kobulnicky

*Department of Physics & Astronomy
University of Wyoming
Laramie, WY 82071
Electronic Mail: chipk@uwyo.edu*

Andrew C. Phillips,

*University of California, Santa Cruz
Lick Observatory/Board of Studies in Astronomy
Santa Cruz, CA, 95064
phillips@ucolick.org*

Revised draft of 28 April 2003

ABSTRACT

We develop a prescription for estimating the interstellar medium oxygen abundances of distant star-forming galaxies using the ratio $EW R_{23}$ formed from the equivalent widths of the [O II] $\lambda 3727$, [O III] $\lambda\lambda 4959, 5007$ and $H\beta$ nebular emission lines. This $EW R_{23}$ approach essentially identical to the widely-used R_{23} method of Pagel *et al.* (1979). Using data from three spectroscopic surveys of nearby galaxies, we conclude that the emission line equivalent width ratios are a good substitute for emission line flux ratios in galaxies with active star formation. The RMS dispersion between $EW R_{23}$ and the reddening-corrected R_{23} values is $\sigma(\log R_{23}) \leq 0.08$ dex. This dispersion is comparable to the emission-line measurement uncertainties for distant galaxies in many spectroscopic galaxy surveys, and is smaller than the uncertainties of $\sigma(O/H) \sim 0.15$ dex inherent in strong-line metallicity calibrations. Because equivalent width ratios are, to first order, insensitive to interstellar reddening, emission line equivalent width ratios may actually be superior to flux ratios when reddening corrections are not available. The $EW R_{23}$ method presented here is likely to be most useful for statistically estimating the mean metallicities for large samples of galaxies to trace their chemical properties as a function of redshift or environment. The approach developed here is used in a companion paper (Kobulnicky *et al.* 2003) to measure the metallicities of star-forming galaxies at $z = 0.2 - 0.8$ in the Deep Extragalactic Evolutionary Probe spectroscopic survey of the Groth Strip.

Subject headings: ISM: abundances — ISM: H II regions — galaxies: abundances — galaxies: fundamental parameters — galaxies: evolution — galaxies: starburst

1. Introduction

Abundances of chemical elements in galaxies are commonly measured using the emission lines emitted by astrophysical nebulae (e.g., see Osterbrock 1989). Recombination lines of hydrogen (e.g., the Balmer series) or helium and forbidden lines of singly and doubly ionized carbon, nitrogen, oxygen, neon, and sulfur are among the strongest observable lines in the visible and ultraviolet spectrum. The relative strengths of each emission line, combined with some knowledge of the temperature and density of the nebulae, provide information about the relative and absolute abundances of each ion. Chemical analyses of individual nebulae have been used to test nucleosynthesis models of stars, the chemical evolutionary history of galaxies, and nucleosynthesis in the big bang (review by Aller 1990; Pagel 1998). Even integrated spectra of entire galaxies may be used to estimate the overall degree of chemical enrichment of a galaxy (Kobulnicky, Kennicutt, & Pizagno 1998).

Observational techniques sometimes permit the relative fluxes of emission lines from galaxies to be measured with a high degree of precision. However, in the current generation of wide-field galaxy surveys on multi-object spectrographs, flux calibration is frequently problematic due to unfavorable observing conditions or instrumental effects such as a variation in system response over the field of view. For such surveys, it is still desirable to extract chemical information from the data, where possible. In this paper we explore the possibility of estimating mean gas-phase oxygen abundances for galaxies based the *equivalent widths* (rather than fluxes) of strong Balmer $H\beta$ recombination line and forbidden [O II] and [O III] emission lines. Our approach is to develop the method from basic principles, and to test and empirically calibrate it using three spectroscopic galaxy datasets, and in the end compare the oxygen abundances derived from traditional line fluxes and flux ratios to results using only the equivalent widths and equivalent width ratios. We also assess the applicability of this method to measuring abundances for a particular set of intermediate-redshift galaxies observed as part of the Deep Extragalactic Evolutionary Probe (DEEP) spectroscopic survey in the Groth Strip (DGSS) presented in a companion paper, Kobulnicky *et al.* (2003; Ke03).

2. Gas-phase Oxygen Abundance Measurements from Emission Lines

Osterbrock (1989) reviews the standard techniques for measuring chemical abundances in astrophysical nebulae from the fluxes and flux ratios of nebular emission lines. The most direct and reliable techniques involve measuring a suite of temperature-sensitive and density-sensitive line ratios to determine the physical conditions of the plasma. In the absence of high signal-to-noise data measuring temperature-sensitive line ratios (e.g., [O III] $\lambda 4363$ /[O III] $\lambda 5007$), the default diagnostic for measuring the oxygen abundance of ionized nebulae has become the ratio of strong oxygen emission lines $R_{23} \equiv (I_{3727} + I_{4959} + I_{5007})/I_{H\beta}$ (Pagel *et al.* 1979). Subsequently, many authors have developed formulations relating this strong line ratio to the gas-phase oxygen abundance (e.g., Edmunds & Pagel 1984; McCall, Rybski & Shields 1985; Dopita & Evans 1986; McGaugh 1991).

Other authors (Kobulnicky, Kennicutt, & Pizagno 1998; KKP) have shown that this approach is valid even when applied to galaxies as a whole. Even when the signal to noise ratio of these lines is as low as 8:1 or when a spectroscopic observation encompasses a range of metallicities and ionization conditions within a galaxy, this ratio provides a rough, but reliable, estimate of the mean gas-phase oxygen abundance when used in conjunction with the appropriate calibration relating R_{23} to O/H . At this signal-to noise ratio, the associated uncertainty on the oxygen abundance due to line measurement error is typically comparable to the uncertainty due to the calibration of the R_{23} vs. O/H relationship: ~ 0.15 dex. In this paper we show that the uncertainty introduced by substituting emission line equivalent widths is less than these other sources of uncertainty, and thereby establish a new method for measuring interstellar medium oxygen abundances.

3. Justification of Equivalent Width Method

The original R_{23} method involves line ratios, so we consider the effects of using equivalent width ratios in place of flux ratios. For generality, we include the effects of reddening in the discussion. First, the equivalent width can be written as

$$W_\lambda = \frac{F_{\lambda 1}}{F_{C\lambda 1}}, \quad (1)$$

where F_λ represents the line flux and $F_{C\lambda}$ is the underlying continuum flux. The fluxes do not need to be calibrated, since the calibration affects both quantities equally. The dereddened, calibrated flux value for a line, I_λ , or continuum, F_λ^0 , is given by

$$I_\lambda = F_\lambda^0 = F_\lambda \times 10^{c(1+f(\lambda))}, \quad (2)$$

where c is the logarithmic attenuation at $H\beta$ and $f(\lambda)$ is a function describing the reddening curve, according to the prescription of Seaton (1979). Combining these leads to a general line ratio formulation of

$$\frac{I_{\lambda 1}}{I_{\lambda 2}} = \frac{W_{\lambda 1} F_{C\lambda 1}}{W_{\lambda 2} F_{C\lambda 2}} 10^{c(f(\lambda 1)-f(\lambda 2))} = \frac{W_{\lambda 1}}{W_{\lambda 2}} \alpha, \quad (3)$$

where we group all the continuum and reddening terms into the factor α . Note that the continuum will be attenuated by an amount characterized by c^* , and reddened by (presumably) the same reddening law. Thus,

$$\alpha = \frac{F_{C\lambda 1}^0}{F_{C\lambda 2}^0} 10^{(c-c^*)(f(\lambda 1)-f(\lambda 2))}. \quad (4)$$

The factor α contains two unknowns, the ratio of the dereddened continuum fluxes, which depends on the underlying stellar population, and the difference in the attenuation of the emitting gas and the continuum light. Note that values of c can range from 0 to quite large for individual HII regions, although large values are severely deweighted in the average over an entire galaxy.

Typical derived values are in the range 0–1, with a median value around 0.3 (McCall *et al.* 1985; Oloffson 1995). Values of c^* can be estimated from the relation $c^* = 1.47E_{B-V}$ from Seaton. For E_{B-V} in a typical range of 0–0.2, $c^* \sim 0$ –0.3. We would expect some correlation of c and c^* , and also we expect $(c - c^*) \geq 0$.

Let us now consider the specific line ratios of interest for the R_{23} method. The first is $I_{[O\ III]}/I_{H\beta}$. For the purposes of reddening, we adopt the wavelength of the stronger [O III] $\lambda 5007$ line. The value of α in this case is

$$\alpha = \frac{F_{C5007}^0}{F_{C4861}^0} 10^{(c-c^*)(-0.034)}. \quad (5)$$

Due to the proximity of these emission lines in wavelength, we expect the flux ratios of the underlying stellar population to be very close to unity. Similarly, for realistic $0 < c - c^* < 1$, the reddening factor will be 1 to 0.92. Thus, for this line ratio, $\alpha \simeq 1$, and we will ignore it in further discussion. To a very good approximation,

$$\frac{I_{[O\ III]}}{I_{H\beta}} = \frac{W_{[O\ III]}}{W_{H\beta}}. \quad (6)$$

The second ratio, $I_{[O\ II]}/I_{H\beta}$, is more problematic; for these lines,

$$\alpha = \frac{F_{C3727}^0}{F_{C4861}^0} 10^{(c-c^*)(0.255)}. \quad (7)$$

In principle, we could estimate α from a detailed spectral analysis of the flux-calibrated, integrated stellar spectrum and Balmer line ratios, but for faint, galaxies with redshifts $z > 0.3$ we will have neither the signal-to-noise nor access to the $H\alpha$ line in order to do this. In practice, we need to adopt a constant average value of α .

Galaxy light tends to be dominated by A main sequence and G and K giants (e.g., Morgan & Mayall 1957; Pritchett 1977; Kobulnicky & Gebhardt 2000), and assuming an underlying stellar spectrum composed of a linear combination of these two spectral types implies that the dereddened flux ratio of the continuum ranges from ~ 1 for late-B stars to ~ 0.4 for mid-G giants to ~ 0.2 for early-K giants (although galaxies whose $\lambda 3727$ flux is dominated by K stars is unlikely to have any line emission from star formation). Examining the spectra in Kennicutt (1992b) shows the $\lambda 3727$ -to- $\lambda 4861$ ratio of the continuum fluxes in galaxies with obvious emission lines ranging from ~ 0.4 –1.0; if these were dereddened the range would shift upwards and might possibly narrow somewhat.

On the other hand, the reddening correction ranges from 1 to 1.8 for realistic values of c and c^* , with a typical likely difference $c - c^* \sim 0.3$ giving a reddening factor of ~ 1.2 . Combining the two factors leads to an expected value of $\alpha \sim 0.84 \pm 0.3$. This average value for α differs from unity by less than 0.1 dex.

We find the R_{23} measure can now be expressed

$$R_{23} = \log \frac{I_{[OII]} + I_{[OIII]}}{I_{H\beta}} = \log \frac{\alpha W_{[OII]} + W_{[OIII]}}{W_{H\beta}}. \quad (8)$$

Not surprisingly, the R_{23} measured using equivalent widths and a constant value of α will be most in error when [OII] dominates O[III].

The final line ratio of interest is the ionization parameter, and it is easy to see that

$$\frac{I_{[OIII]}}{I_{[OII]}} \simeq \frac{W_{[OIII]}}{\alpha W_{[OII]}}. \quad (9)$$

This ratio is probably the easiest means to empirically estimate an average value for α .

4. Data Selection and Analysis

The thesis of this paper is that even when the line *flux* ratio R_{23} is not available, a corresponding ratio of *equivalent widths* can still provide an estimate of the oxygen abundance. This ratio of equivalent widths is given by

$$EWR_{23} \equiv \frac{EW([O II]\lambda 3727) + EW([O III]\lambda 4959) + EW([O III]\lambda 5007)}{EW(H\beta)}. \quad (10)$$

At the simplest level, EWR_{23} contains neither corrections for interstellar reddening nor absorption by atmospheres of the stellar population. To test the suitability of EWR_{23} in place of R_{23} we compiled three sets of spatially-integrated (i.e., global) emission-line spectra of nearby galaxies. The first set consists of 16 objects from the 55-object spectroscopic galaxy atlas of Kennicutt (1992a,b; K92) plus six additional emission-line objects from KKP. We refer to this sample as the K92+ sample. The K92+ spectra are produced by drifting a longslit across each galaxy and have spectral resolutions of 5-7 Å (K92) and 3 Å (KKP). The 16 K92 galaxies in our subsample are the strongest emission-line objects where global metallicity measurements are possible. The full set of K92 galaxies represents a range of morphological types from Sa to Im, but it includes only the bright galaxies of each type. As a second local sample, we culled 98 objects with measurable $H\beta$, [O III] and [O II] emission lines from the 198-galaxy Nearby Field Galaxy Survey (Jansen *et al.* 2000a,b; NFGS). The full NFGS sample is selected from the CfA redshift catalog (Huchra *et al.* 1983). These spectra have a resolution of 6 Å and include a larger range of luminosity ($-14 < M_B < -22$) and surface brightnesses than K92+ while spanning morphological types. The K92+ objects have a higher fraction of star-forming galaxies (objects with strong emission lines) compared to the NFGS sample. As a third local sample, we used emission-line selected galaxies in the Kitt Peak National Observatory Spectroscopic Survey (KISS; Salzer *et al.* 2000). KISS is a large-area objective prism survey of local ($z < 0.09$) galaxies selected by strong $H\alpha$ emission, and thus, preferentially contains objects with active star formation. From a list of ~ 519 KISS galaxies

with high-quality slit spectroscopy (Melbourne & Salzer 2002), we removed 396 galaxies lacking [O II] measurements, leaving 123 galaxies. This analysis makes use of KISS line strengths obtained during followup longslit spectroscopy with 5–8 Å resolution (Salzer *et al.* 2003).

In summary, the 22 K92+, 98 NFGS, and 123 KISS galaxies were selected from their larger parent samples because of strong emission lines suitable for nebular metallicity measurement. Following KKP, we chose only galaxies with detectable [O II]λ3727, [O III]λ4959, [O III]λ5007, and Hβ emission lines. Only galaxies where all four emission lines were measured with a S/N of 8:1 or greater were retained. This selection criterion preferentially includes galaxies with high equivalent width lines, but it also includes galaxies with low equivalent width lines where the continuum is smooth and well-measured.

For each galaxy in the K92+ sample we measured the emission-line fluxes and equivalent widths manually using Gaussian fits. For the NFGS and KISS surveys, we adopted the published emission-line fluxes and equivalent widths. Dereddened emission-line fluxes were computed for all three samples by comparing the observed $F_{H\alpha}/F_{H\beta}$ ratios to theoretical ratios.¹ The line fluxes are dereddened using the law of Seaton (1979) as parameterized by Howarth (1983) and as described in Kobulnicky & Skillman (1996). We did not correct the Balmer emission lines for underlying stellar absorption. The effects of Balmer absorption by the stellar population are discussed in Section 5.3

While the K92+KKP sample consists entirely of starforming galaxies, several low-level AGN are known to exist in the NFGS. These four objects are not included in the our subsample. The 123 KISS galaxies included here do not contain any AGN, as they were selected to be conventional starforming galaxies based on analysis high-quality spectroscopic observations (Salzer 2003). In any case, the presence of AGN among the samples would not have a significant bearing on the results of this paper since we are interested in comparing observable properties of emission lines rather than deriving physical quantities such as density or metallicity which are sensitive to the nature of the ionizing source.

5. Analysis of Emission Line Quantities

5.1. [O II] and [O III] Equivalent Widths versus Fluxes

Figure 1 compares the oxygen and hydrogen emission-line flux ratios to equivalent width ratios as a function of emission line strength and $B - V$ color for the K92+ and NFGS samples. Solid symbols denote the Nearby Field Galaxy Sample while crosses denote the K92+ galaxies. The upper left panel compares the ratio of dereddened [O II] to Hβ fluxes, $I_{[O II]}/I_{H\beta}$, versus the ratio of [O II] to Hβ equivalent widths, $EW_{[O II]}/EW_{H\beta}$. A solid line marks the 1-to-1 correspondence.

¹ $I_{H\alpha}/I_{H\beta} = 2.75\text{--}2.86$ for wide temperature range, e.g., (Hummer & Storey 1987). Here we assumed fixed electron temperature of 12,000 K so that $I_{H\alpha}/I_{H\beta} = 2.85$.

There is a good correlation between the two quantities, indicating that strong-line equivalent widths are a good surrogate for dereddened line fluxes. The RMS deviation from the 1-to-1 correspondence is $\sigma(\log[EW_{[O\ II]}/EW_{H\beta}]) = 0.11$ dex for the combined K92+NFGS samples. Similarly, the panel at top center shows the $I_{[O\ III]}/I_{H\beta}$ versus $EW_{[O\ III]}/EW_{H\beta}$ ratios and indicates that equivalent widths are a good surrogate for dereddened line fluxes. The RMS deviation from the 1-to-1 correspondence is $\sigma(\log[EW_{[O\ III]}/EW_{H\beta}]) = 0.05$ dex for the combined K92+NFGS samples. The panel at upper right shows the histogram of $EW_{[O\ II]}/EW_{H\beta}$ and $EW_{[O\ III]}/EW_{H\beta}$ distributions for the DGSS galaxies (Ke03) galaxies. The ratios observed in Groth Strip galaxies fall within the range where the relations between flux ratios and EW ratios are well-behaved, suggesting that the EW_{R23} approach could be used to estimate oxygen abundances of this sample.

The lower panels of Figure 1 show residuals from the 1-to-1 line as a function of EW and galaxy color. The K92+ galaxies have very small residuals in the middle column which compares [O III] to $H\beta$ ratios. The excellent correspondence of [O III] fluxes to equivalent widths may be easily understood since the [O III] $\lambda\lambda 4959, 5007$ lines are close in wavelength to $H\beta$ so that neither changes in the underlying galaxy continuum light nor relative extinction will alter this ratio. The K92+ and NFGS galaxies have small, slightly-systematic residuals in the left column which compares the [O II] to $H\beta$ ratios. We attribute the larger residuals in the [O II] comparison in the left column to uncertainties in the reddening correction, and possibly a systematic overestimate of the reddening correction to the [O II] $\lambda 3727$ flux due to low spectral resolution in the K92 atlas. The NFGS, by comparison, shows systematic trends in the residuals with B-V color, with $EW_{[O\ II]}$ and with $EW_{H\beta}$. The galaxies with the largest residuals are also the reddest. They have very low $H\beta$ equivalent widths, and they have the largest $EW_{[O\ II]}/EW_{[O\ III]}$ ratios. Such objects may be understood to be the galaxies with the lowest rates of star formation per unit luminosity and the oldest stellar populations. For these objects, the line ratios become increasingly uncertain as the line strengths become weak and the (uncorrected) effect of underlying Balmer absorption by the stellar population begins to be a dominant source of scatter.

The right column of histograms in Figure 1 shows the distribution of colors and EW ratios for galaxies in the DGSS selected for chemical analysis in our companion paper (Kobulnicky *et al.* 2003). The selected DGSS galaxies have strong emission lines and tend to be most similar to the K92+ and KISS galaxies, having blue colors, small $EW_{[O\ II]}/EW_{[O\ III]}$ ratios, and large $EW_{H\beta}$ in comparison the NFGS. These characteristics suggest that, like the K92+ and NFGS galaxies with these properties, the DGSS galaxies will exhibit a close correlation between the emission line equivalent width and flux ratios, facilitating chemical abundance analysis.

In Figure 2 shows the same comparison as Figure 1 but for the KISS and K92+ samples. The upper left panel compares the ratio of dereddened [O II] to $H\beta$ fluxes, $I_{[O\ II]}/I_{H\beta}$, versus the ratio of [O II] to $H\beta$ equivalent widths, $EW_{[O\ II]}/EW_{H\beta}$. A solid line marks the 1-to-1 correspondence. There is a good correlation between the two quantities, indicating that strong-line equivalent widths are a good surrogate for dereddened line fluxes. The RMS deviation from the 1-to-1 correspondence is $\sigma(\log EW_{[O\ II]}/EW_{H\beta}) = 0.15$ dex for the combined K92+KISS samples. Similarly, the

panel at top center shows the $I_{[O\ III]}/I_{H\beta}$ versus $EW_{[O\ III]}/EW_{H\beta}$ ratios and indicates that equivalent widths are a good surrogate for dereddened line fluxes. The RMS deviation from the 1-to-1 correspondence is $\sigma(\log[EW_{[O\ II]}/EW_{H\beta}]) = 0.04$ dex for the combined K92+KISS samples.

The lower panels of Figure 2 show residuals from the 1-to-1 line as a function of EW and galaxy color. The middle column shows very small and non-systematic residuals, indicating excellent correspondence between [O III] equivalent widths and fluxes for all KISS galaxy colors and line ratios. However, the left column shows significant dispersion of 0.15 dex between $\log EW_{[O\ II]}/EW_{H\beta}$ and $\log I_{[O\ II]}/I_{H\beta}$. The residuals are not correlated with galaxy color or EW, suggesting that measurement errors and/or uncertainties in the reddening correction are responsible for the dispersion.

The right column of histograms in Figure 2 shows the distribution of colors and EW ratios for galaxies in the DGSS selected for chemical analysis in our companion paper (Kobulnicky *et al.* 2003).

5.2. $EW R_{23}$ versus R_{23}

A more direct test of the suitability of emission line equivalent width ratios for abundance analysis can be achieved by comparing the quantity $EW R_{23}$ with R_{23} for the same three local galaxy samples. Figure 3 (upper left panel) shows the comparison between R_{23}^* and $EW R_{23}$ for K92+ and NFGS galaxies constructed from the raw fluxes and equivalent widths. R_{23}^* denotes the value of R_{23} *without* correcting line fluxes for reddening. A solid line illustrates a 1-to-1 correspondence. The lower rows in the left column of Figure 3 show residuals from the 1-to-1 correspondence as a function of $EW_{H\beta}$, $EW_{[O\ II]}$, $EW_{[O\ II]}/EW_{[O\ III]}$ and galaxy $B-V$ color. The correlation between R_{23}^* and $EW R_{23}$ is strong but has considerable scatter. Formally, the RMS dispersion from the 1-to-1 relation is $\sigma(\log[R_{23}^*]) = 0.12$ dex for the combined K92+NFGS samples.

The correlation is strongest for objects in the K92+ sample and for objects with large values of R_{23}^* . Deviations from 1-to-1 are greatest for objects in the NFGS sample which have low $EW_{H\beta}$, high $EW_{[O\ II]}/EW_{[O\ III]}$ ratios, and red colors. These systematic residuals may be understood as a consequence of the lack of corrections for extinction. [O II] $\lambda 3727$ is significantly affected by extinction compared to the $H\beta$ and [O III] lines. The measured [O II] flux is a lower limit to the true unextincted intensity whereas the measured [O II] equivalent width should be unaffected by extinction provided that the extinction toward the gas and stars are similar². The strong systematic residuals with $B-V$ color seen in the lower left panel is a most likely a consequence uncorrected extinction, since redder galaxies are often those with greater extinction.

In the middle column of Figure 3 we show a similar comparison of $EW R_{23}$ with R_{23} , where R_{23} has been corrected for reddening using the theoretical Balmer decrement. Here the correlation is

²See Calzetti, Kinney, & Storchi-Bergmann (1994) for evidence that this assumption is sometimes invalid.

much stronger. The strong correlation between galaxy color and residuals seen in left column is now mostly gone, suggesting that the [O II] line fluxes have been successfully corrected for reddening. The RMS dispersion from the 1-to-1 relation is $\sigma(\log[R_{23}]) = 0.07$ dex for the combined K92+NFGS samples. The ratio of equivalent widths is a good substitute for the reddening-corrected R_{23} ratio. Use of equivalent widths may even be superior to line ratios if the reddening corrections are not known, as in the case of galaxies for which the $H\alpha/H\beta$ ratio is not available (typically true for redshifts $z > 0.3$). In the presence of reddening, the EW of the [O II] line is unchanged because both the continuum and line flux are suppressed in equal amounts if the reddening toward stars and gas is similar. The residuals in the lower panels of column 2 are mostly symmetric about zero, with the largest scatter again occurring for objects with very low values of $EW(H\beta)$. Some of the systematic residuals are probably also caused by varying continuum shapes, especially among the NFGS, which affect the equivalent widths of the [O II] lines in a systematic manner which is related to galaxy color and the average age of the stellar population. In any case, the RMS of 0.07 dex in R_{23} will often be on the same order as, or even less than the statistical measurement uncertainties on the strong line equivalent widths in high-redshift spectroscopic surveys, even when the signal-to-noise of the emission line equivalent widths is as low as 8:1.

The right column of Figure 3 shows the distribution of the 66 galaxies from the DGSS selected for chemical analysis in Kobulnicky *et al.* (2003). The range of $EW_{R_{23}}$, $EW_{H\beta}$, $EW_{[O II]}$, and $EW_{[O II]}/EW_{[O III]}$ among the sample galaxies covers the range over which the local calibration galaxies show a well-behaved relationship between $EW_{R_{23}}$ and R_{23} . The good correlation ($\sigma_{23}=0.08$ dex) between R_{23} and $EW_{R_{23}}$ in the local samples provides confidence that measuring rough ISM oxygen abundances in large surveys of distant galaxies is feasible even when only equivalent widths are recorded.

Figure 4 shows a comparison of $EW_{R_{23}}$ with R_{23}^* and R_{23} for the K92+ and KISS galaxy samples. The left column shows the comparison of $EW_{R_{23}}$ with R_{23}^* and the associated residuals from the 1-to-1 correspondence. There is a good correlation between $EW_{R_{23}}$ with R_{23}^* in the upper left panel. The RMS dispersion from the 1-to-1 relation is $\sigma(\log[R_{23}]) = 0.11$ dex for the combined K92+KISS samples. The left column shows systematic residuals with galaxy color and line strength indicating that reddening is significant for some galaxies. The center column shows the comparison of $EW_{R_{23}}$ with R_{23} and the associated residuals as a function of EW and galaxy color. The residuals for the KISS galaxies are now slightly smaller and much less systematic after application of a reddening correction. The RMS dispersion from the 1-to-1 relation is $\sigma(\log[R_{23}]) = 0.09$ dex for the combined K92+KISS samples. The residuals are larger than for the K92+ and NFGS objects, but the KISS galaxies do not show the systematics with galaxy color or EW which the NFGS galaxies exhibit. The increased scatter in R_{23} may be traced to the increased scatter in the [O II] lines seen in Figure 2. The lack of systematic residuals is probably a result of the relative homogeneity of the KISS sample. KISS galaxies have stronger emission lines and do not include the diversity of more quiescent galaxies with older stellar populations found in the NFGS.

5.2.1. Effects of Stellar Balmer Absorption

Ideally, the quantity R_{23} from which a metallicity is derived should be computed using an $H\beta$ line strength which has been corrected for both interstellar reddening *and* absorption by atmospheres of the underlying stellar population. In practice, the amount of underlying absorption is difficult to measure even under ideal circumstances with high signal-to-noise data. Spectra of distant galaxies frequently lack the signal-to-noise necessary to measure multiple Balmer lines and correct simultaneously for extinction and Balmer absorption in a self-consistent fashion. For galaxies with strong emission lines due to active star formation (i.e., $EW_{H\beta} > 25 \text{ \AA}$), a correction of a few \AA to the $H\beta$ line will have a small impact on the derived R_{23} or $EW R_{23}$. However, in galaxies dominated by older stellar populations with weak emission lines, R_{23} or $EW R_{23}$ will depend sensitively on the correction for Balmer absorption.

Until this point in the analysis, we have not made any corrections for stellar Balmer absorption. The effect of underlying Balmer absorption (specifically the amount of absorption in the $H\beta$ line, $EW_{H\beta}(abs)$) will depress the measured $F_{H\beta}$ and $EW_{H\beta}$. This leads to systematically large R_{23} or $EW R_{23}$, and systematically low oxygen abundances for objects on the upper (metal-rich) branch of the empirical calibrations.

The impact of stellar absorption can be assessed using Figure 5. Using the K92+ galaxies, we performed a self-consistent reddening and stellar absorption correction for each galaxy. The upper left panel compares the raw $EW R_{23}$ ratio with the quantity R_{23}^+ which includes the corrections for reddening and stellar absorption. The correlation between $EW R_{23}$ and R_{23}^+ is modest, with a dispersion of $\sigma(R_{23}^+) = 0.14$ dex and a systematic offset of 0.06 dex. The lower panels illustrate the nature of the residuals as a function of galaxy color and EW. As might be expected, galaxies with the lowest $EW_{H\beta}$ are the most deviant, while galaxies with $EW_{H\beta} > 20$ show a much smaller dispersion. A more logical approach is also to add a correction to $EW_{H\beta}$ for the underlying stellar absorption, forming a new quantity $EW R_{23}^+$. Galaxies with the lowest $EW_{H\beta}$ are affected most by this correction. A 2 \AA correction to $EW_{H\beta}$ was chosen because it was the mean correction needed to produce R_{23}^+ , and is consistent with mean corrections found for other galaxies (e.g., McCall *et al.* 1985; Olofsson 1995). The center top panel shows $EW R_{23}^+$ plotted against R_{23}^+ . The residuals are now much smaller with $\sigma(R_{23}^+) = 0.08$ dex and a systematic offset of less than 0.01 dex. In the absence of direct measurements of the Balmer absorption due to stellar populations, application of a 2 \AA blanket correction to $EW_{H\beta}$ appears to be prudent.

5.3. The Ionization Parameter Quantity $[\text{O III}]/[\text{O II}]$

Modern calibrations relating R_{23} to oxygen abundance include a measure of the ionization parameter, such as $O_{32} \equiv (F_{4959} + F_{5007})/F_{3727} = F_{[\text{O III}]} / F_{[\text{O II}]}$ as a second parameter (e.g., McGaugh 1991; Pilyugin 2001). We test the suitability of using a quantity $EW_{[\text{O III}]} / EW_{[\text{O II}]}$ in place of $F_{[\text{O III}]} / F_{[\text{O II}]}$ in Figure 6. K92+ galaxies appear as crosses and the NFGS galaxies

appear as solid symbols. The upper left panel shows the correlation between $EW_{[O\ III]}/EW_{[O\ II]}$ and $F_{[O\ III]}/F_{[O\ II]}$, where F denotes line strengths that have not been corrected for reddening. Although the correlation is strong, the residuals in the lower rows are large and strongly systematic with galaxy color and emission line EW . The top middle panel shows the correlation between $EW_{[O\ III]}/EW_{[O\ II]}$ and $I_{[O\ III]}/I_{[O\ II]}$, where I denotes line strengths that have been corrected for reddening. The correlation is now much stronger and less systematic. The RMS dispersion is $\sigma(I_{[O\ III]}/I_{[O\ II]}) = 0.12$ dex. The mean residuals of the two samples are systematic in different directions. The residuals of the K92+ galaxies suggest a systematic reddening overcorrection of the $[O\ II]\ \lambda 3727$ line. The residuals for the NFGS galaxies are still systematic with galaxy color and suggest a reddening undercorrection for the reddest galaxies. The two samples have been analyzed identically, and we have no explanation for the apparent differences. A more rigorous comparison would require re-measuring all of the line strengths and equivalent widths to ensure uniform treatment of the samples. However, electronic spectra for the NFGS and KISS galaxies are not publicly available.

In Figure 7 we show the $EW_{[O\ III]}/EW_{[O\ II]}$ versus $F_{[O\ III]}/F_{[O\ II]}$ and $I_{[O\ III]}/I_{[O\ II]}$ comparisons for the KISS galaxies. The residuals for both the left and center columns are $\sigma(F_{[O\ III]}/F_{[O\ II]}) = 0.15$ dex and $\sigma(I_{[O\ III]}/I_{[O\ II]}) = 0.14$ dex. The lack of improvement with reddening correction is undoubtedly traceable to the large, apparently random, dispersion in the $[O\ II]$ line strengths and EWs of the KISS spectra, as noted in previous figures.

In summary, the $EW_{[O\ III]}/EW_{[O\ II]}$ ratios could be used as a surrogate for $F_{[O\ III]}/F_{[O\ II]}$ ratios as a indicator of the ionization parameter. The residuals are on the order of $0.12 - 0.15$ dex and are sometimes strongly systematic with galaxy color. The mean of the residuals varies considerably from -0.08 dex to 0.12 dex in $EW_{[O\ III]}/EW_{[O\ II]}$ depending on the galaxy sample under study.

6. Discussion and Conclusions

The ratios of the equivalent widths of strong oxygen and hydrogen emission lines from the ionized component of distant galaxies can be used as a measure of the global ISM metallicity via the substitution of $EW R_{23}$ for R_{23} . We recommend the use of $EW R_{23}^+$ where the $EW_{H\beta}$ has been corrected for stellar Balmer absorption assuming a mean correction of $2\ \text{\AA}$. The typical dispersion from the 1-to-1 relation between either $EW R_{23}$ or $EW R_{23}^+$ and the canonical reddening and absorption-corrected R_{23} ratio is $\sigma(R_{23}) = 0.08$ dex. Residuals are somewhat smaller ($\sigma = 0.05$ dex) for galaxies with the largest emission-line equivalent widths (i.e., those having the largest rates of star formation per unit luminosity). The additional uncertainty introduced by translating a set of measured equivalent widths into the traditional R_{23} flux ratio diagnostic is comparable to or less than the typical observational line measurement uncertainties and systematic errors in the R_{23} to O/H calibration which run 0.15 dex in O/H (e.g., Kobulnicky, Kennicutt & Pizagno 1999 for a more detailed discussion of the error budget). We anticipate that the method tested here will be

useful for performing rough chemical abundance estimates in large high-redshift galaxy samples. The approach described here will be most useful in a statistical sense when large numbers of objects are available for study. Possible applications include understanding the overall chemical evolution of star forming galaxies over large intervals of cosmic time (Kobulnicky *et al.* 2003) or assessing the impact of cluster environment and the intracluster medium on the chemical properties of the ISM within galaxies (e.g., Skillman *et al.* 1996).

John Salzer helped make this paper possible by providing the KISS data in tabulated form and by commenting on the manuscript. Detailed comments by an anonymous referee greatly improved the manuscript. We thank Shiela Kannappan for a helpful discussion about the NFGS and Matt Bershadsky for scientific inspiration. H. A. K was supported by NASA through grant #HF-01090.01-97A awarded by the Space Telescope Science Institute which is operated by the Association of Universities for Research in Astronomy, Inc. for NASA under contract NAS 5-26555. This work was also made possible by funding from the National Science Foundation through grant AST-9529098, and NASA through NRA-00-01-LTSA-052.

REFERENCES

- Aller, L. H. 1990, *PASP*, 102, 1097
- Calzetti, D., Kinney, A. L., & Storchi-Bergmann, T. 1994, *ApJ*, 429, 582
- Dopita, M. A., & Evans, I. N. 1986, *ApJ*, 307, 431
- Edmunds, M. G. & Pagel, B. E. J. 1984, *MNRAS*, 211, 507
- Howarth, I. D. 1983, *MNRAS*, 203, 301
- Huchra, J. P., Davis, M., Latham, D., & Tonry, J. 1983, *ApJS*, 52, 89
- Hummer, D. G., & Storey, P. J. 1987, *MNRAS*, 224, 801
- Jansen, R. A., Franx, M., Fabricant, D., & Caldwell, N. 2000a, *ApJS*, 126, 271 (NFGS)
- Jansen, R. A., Fabricant, D., Franx, M., & Caldwell, N. 2000b, *ApJS*, 126, 331
- Kennicutt, R. C. Jr. 1992a, *ApJS*, 79, 255
- Kennicutt, R. C. Jr. 1992b, *ApJ*, 388, 310
- Kobulnicky, H. A., Kennicutt, R. C., & Pizagno, J. 1998, *ApJ*, 514, 544 (KKP)
- Kobulnicky, H. A. & Gebhardt, K. 2000, *AJ*, 119, 1608
- Kobulnicky, H. A., Willmer, C. N. A., Weiner, B. J., Koo, D. C., Phillips, A. C., Faber, S. M., Sarajedini, V. L., Simard, L., & Vogt, N. P. 2003, *ApJ*, 000 (Ke03)
- Kobulnicky, H. A., & Skillman, E. D. 1996, *ApJ*, 471, 211
- McCall, M. L., Rybski, P. M., & Shields, G. A. 1985, *ApJS*, 57, 1 (MRS)

- McGaugh, S. 1991, *ApJ*, 380, 140
- McGaugh, S. 1998, private communication
- Melbourne, J., & Salzer, J. J. 2002, *AJ*, 123, 2302
- Morgan, W. W., & Mayall, N. U. 1957, *PASP*, 69, 291
- Olofsson, K. 1995, *A&AS*, 111, 570
- Osterbrock, D. E. 1989, *Astrophysics of Gaseous Nebulae and Active Galactic Nuclei*, University Science Books:Mill Valley CA
- Pagel, B. E. J. 1998, *Nucleosynthesis and Chemical Evolution of Galaxies*, Cambridge University Press
- Pagel, B. E. J. Edmunds, M. G., Blackwell, D. E., Chun, M. S., & Smith, G. 1979, *MNRAS*, 189, 95
- Pilyugin, L. S., 2001, *A&A*, 369, 594
- Pritchett, C. R. 1977, *ApJS*, 35, 397
- Salzer, J. J. 2003, private communication
- Salzer, J. J. *et al.* 2003, in press
- Salzer, J. J., Gronwall, C., Lipovetsky, V. A.; Kniazev, A., Moody, J. W., Boroson, T. A., Thuan, T. X., Izotov, Y. I., Herrero, J. L., Frattare, L. M. 2000, *AJ*, 120, 80 (KISS)
- Seaton, M. J. 1979, *MNRAS*, 187, 73p
- Skillman, E. D., Kennicutt, R. C., Shields, G. A., & Zaritsky D. 1996, *ApJ*, 462, 147

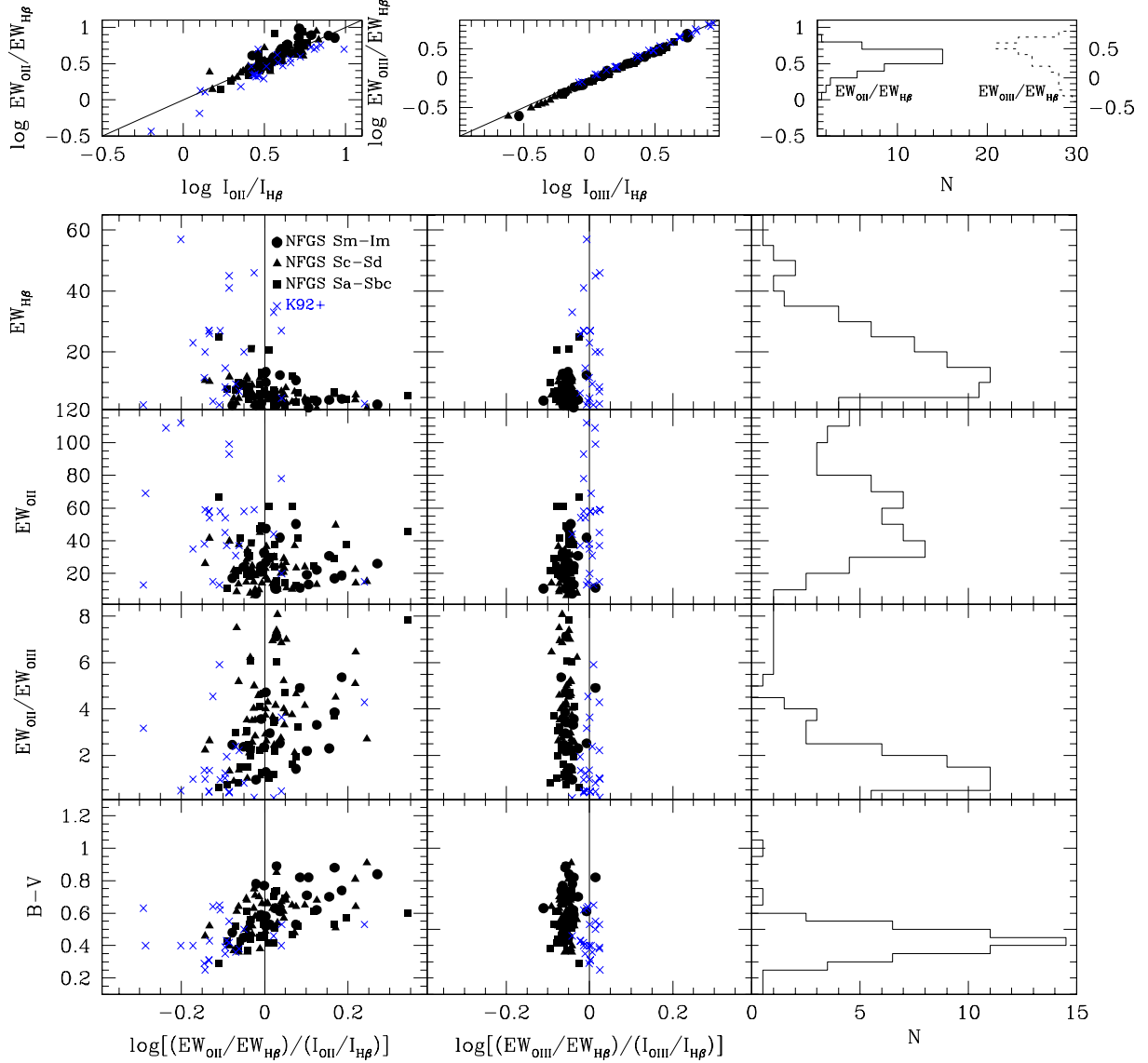


Fig. 1.— Comparison of dereddened emission line fluxes and flux ratios to emission line equivalent widths and EW ratios for galaxies from Kennicutt (1992a,b) and Jansen *et al.* (2000a,b; NFGS). Upper panels show the [O II]/H β flux ratios and EW ratios with a line illustrating the 1-to-1 correspondence. Lower panels show residuals from the 1-to-1 relation as a function of equivalent width and galaxy color. There is generally a strong correlation between flux ratios and EW ratios. Panels showing systematic residuals are discussed in the text. Histograms at right indicate the distribution of emission line equivalent widths and colors for 66 DGSS galaxies analyzed in Kobulnicky *et al.* (2003).

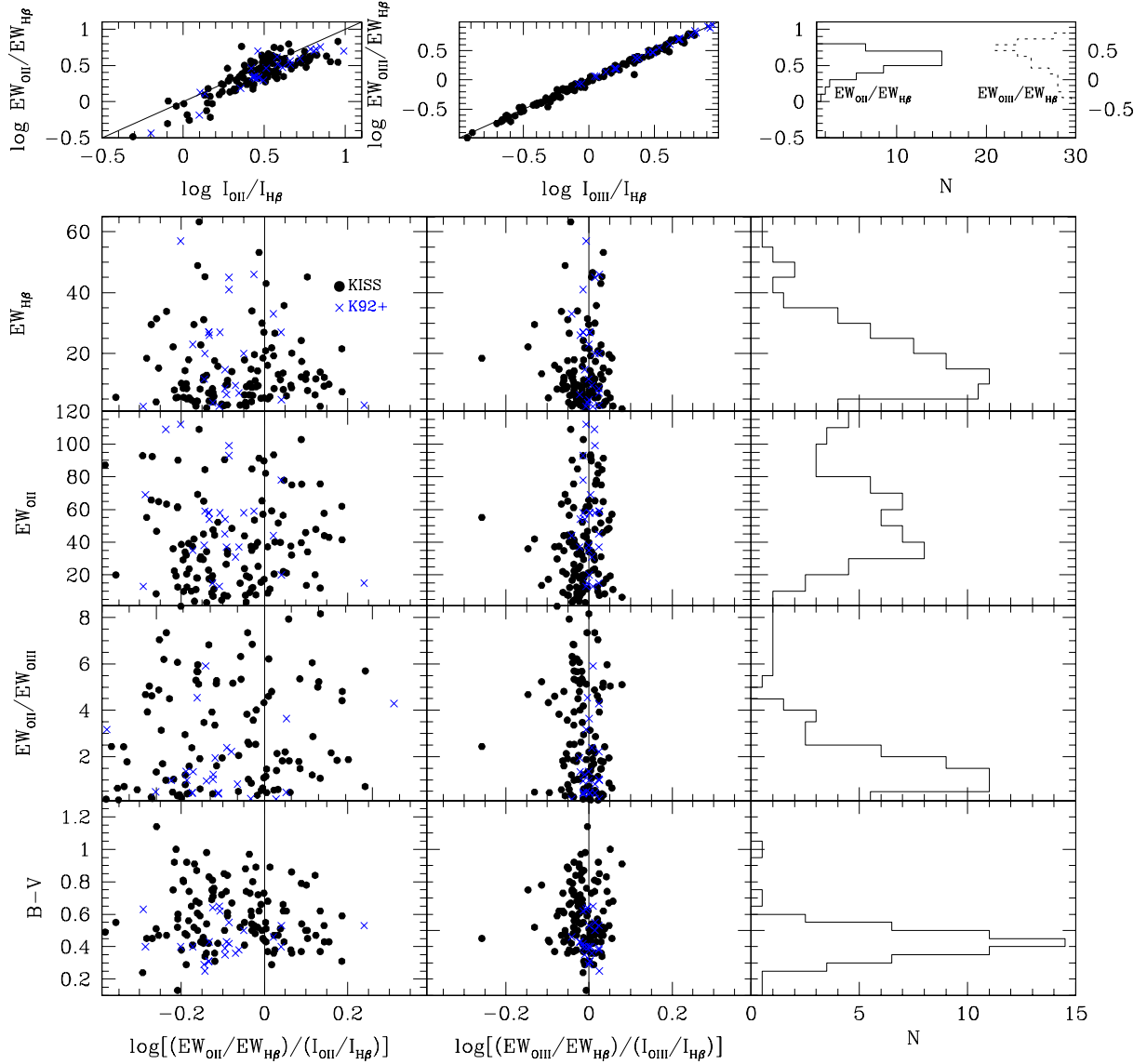


Fig. 2.— Comparison of dereddened emission line fluxes and flux ratios to emission line equivalent widths and EW ratios for galaxies from the K92+ galaxies and the KISS (Salzer *et al.* 2001) emission line galaxy survey. Upper panels show the $[\text{O II}]/\text{H}\beta$ flux ratios and EW ratios with the line illustrating the 1-to-1 correspondence. Lower panels show residuals from the 1-to-1 relation as a function of equivalent width and galaxy color. There is generally a strong correlation between flux ratios and EW ratios. Panels showing systematic residuals are discussed in the text. Histograms at right indicate the distribution of emission line equivalent widths and colors for DGSS galaxies analyzed in Kobulnicky *et al.* (2003).

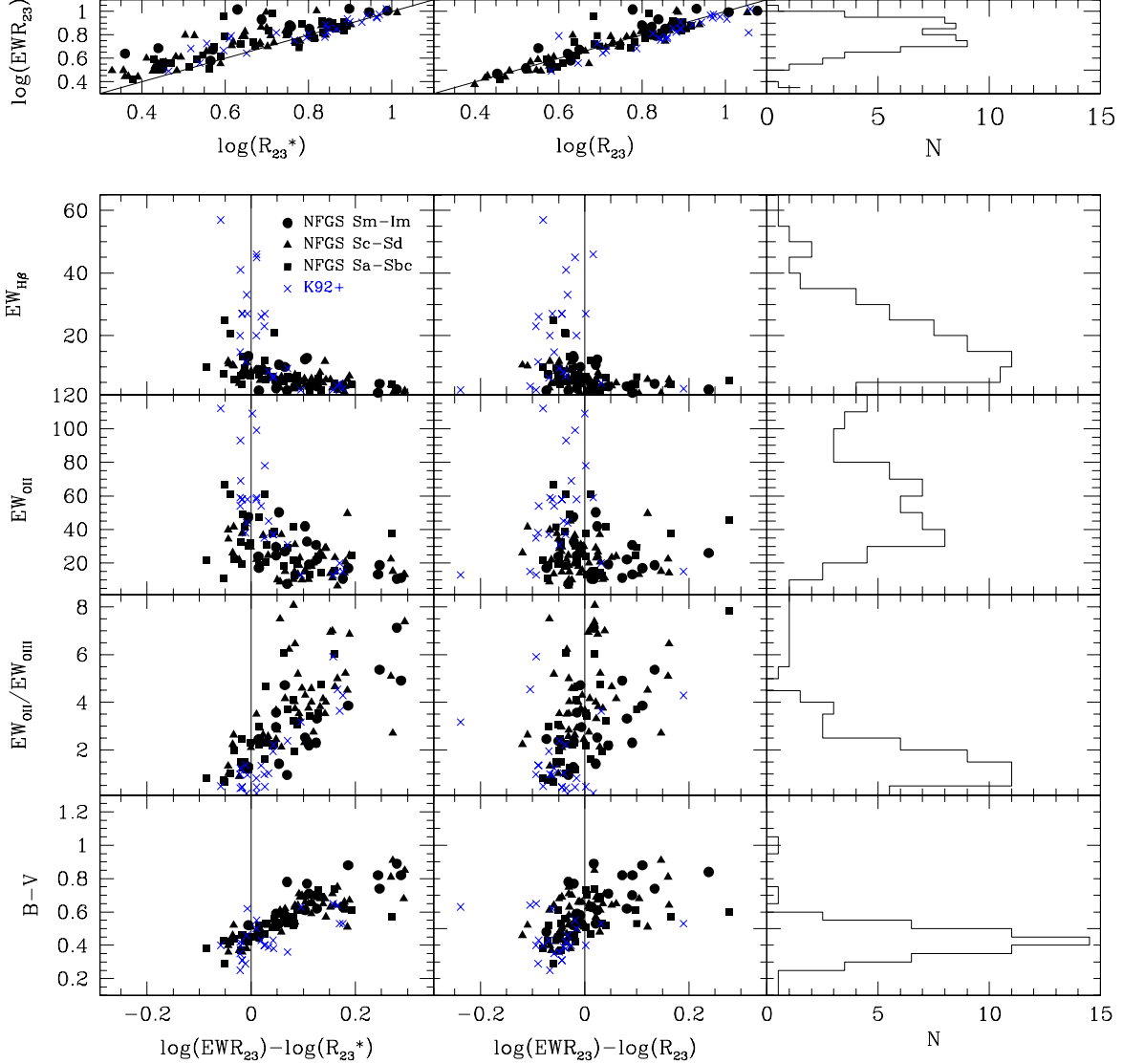


Fig. 3.— Comparison of the quantity R_{23} and R_{23}^* with EWR_{23} . R_{23}^* is R_{23} without correction for reddening. The strong correlation between R_{23}^* and EWR_{23} (upper left panel) is even stronger for R_{23} and EWR_{23} , suggesting that oxygen abundances can be estimated from equivalent width ratios at least as well as from dereddened line fluxes. The RMS dispersion from the 1-to-1 relation is $\sigma(\log[R_{23}]) = 0.07$ dex. Lower panels explore the residuals in the correlation as a function of line strength, line ratio, and galaxy color. *left column*: no correction for extinction or underlying Balmer absorption in either quantity; *middle column*: line fluxes have been corrected for extinction; *right column*: histogram of the distribution of 66 emission-line galaxies selected for analysis from the DGSS showing that the majority of galaxies lie in regimes where the EWR_{23} vs. R_{23} correlation is strong and well-behaved.

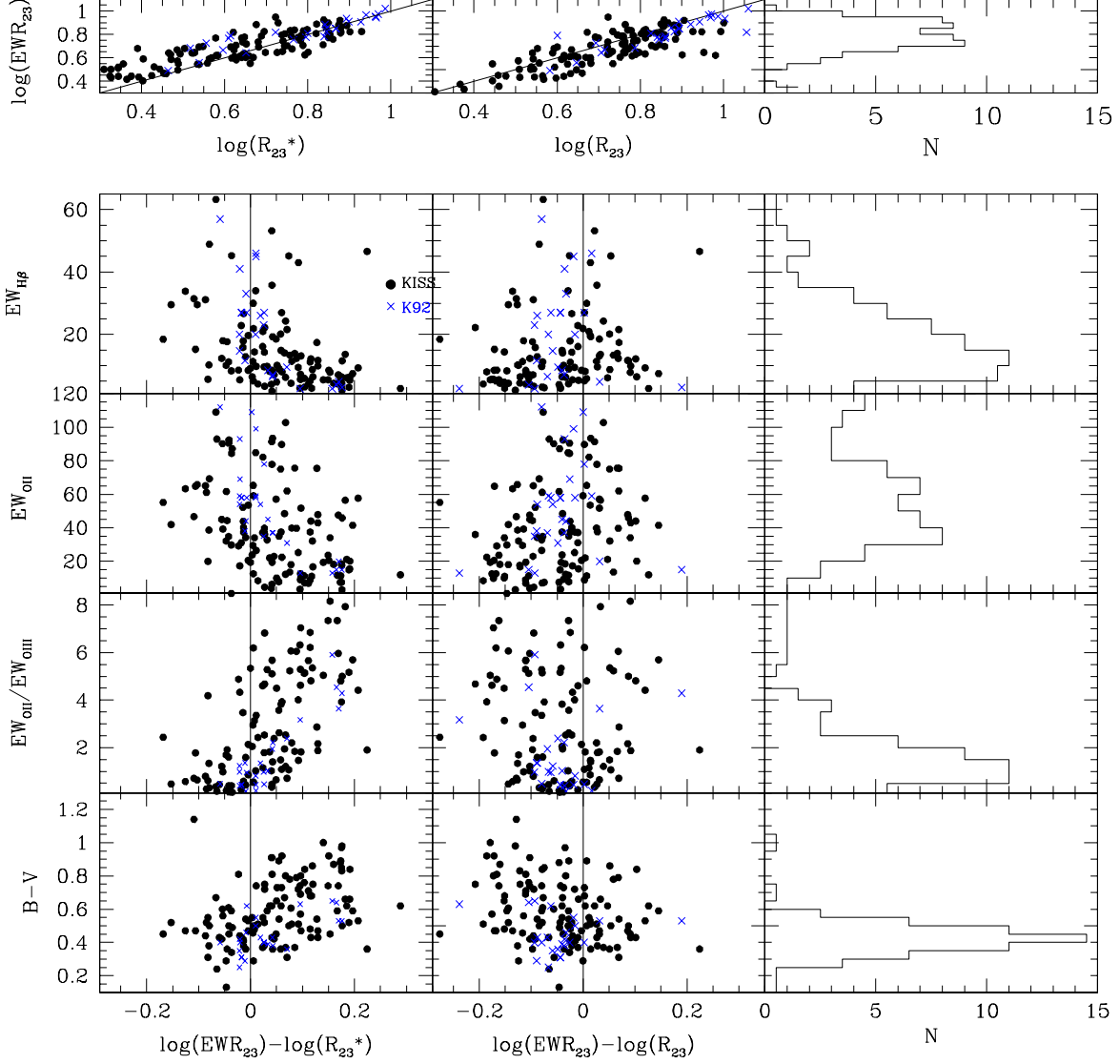


Fig. 4.— Comparison of the quantity R_{23} and R_{23}^* with $EW_{R_{23}}$ for the K92+ and KISS galaxy samples. Upper panels show the excellent correlation between R_{23} and R_{23}^* with $EW_{R_{23}}$. Lower panels show the residuals from the 1-to-1 correspondence as a function of line strength and galaxy color. Residuals are larger, but less systematic, for the KISS galaxies than for the NFGS and K92+ galaxies. As in previous figures, histograms in the right column show the distribution of DGSS galaxies analyzed using this approach in Ke03.

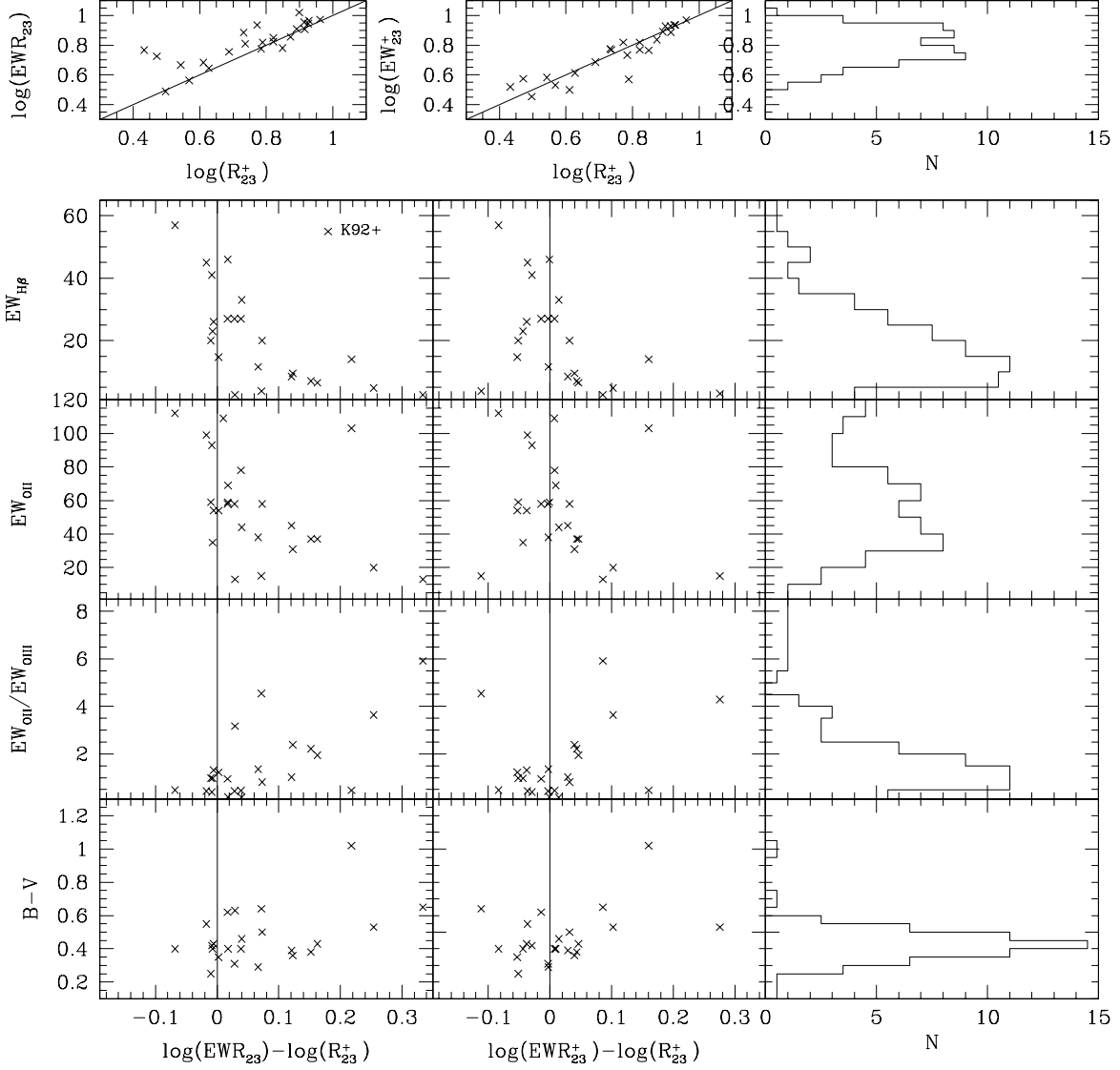


Fig. 5.— Comparison of the quantity R_{23}^+ with EWR_{23} and EWR_{23}^+ for the K92+ galaxies only. EWR_{23}^+ is EWR_{23} where $EW_{H\beta}$ has been increased by 2 \AA to account for stellar absorption. R_{23}^+ is R_{23} with self-consistent corrections for both reddening and stellar Balmer absorption. Upper panels show the correlation between R_{23}^+ and with EWR_{23} and EWR_{23}^+ . Lower panels show the residuals from the 1-to-1 correspondence as a function of line strength and galaxy color. Galaxies with $EW_{H\beta} \leq 15 \text{ \AA}$ are most seriously affected by the lack of correction for stellar absorption.

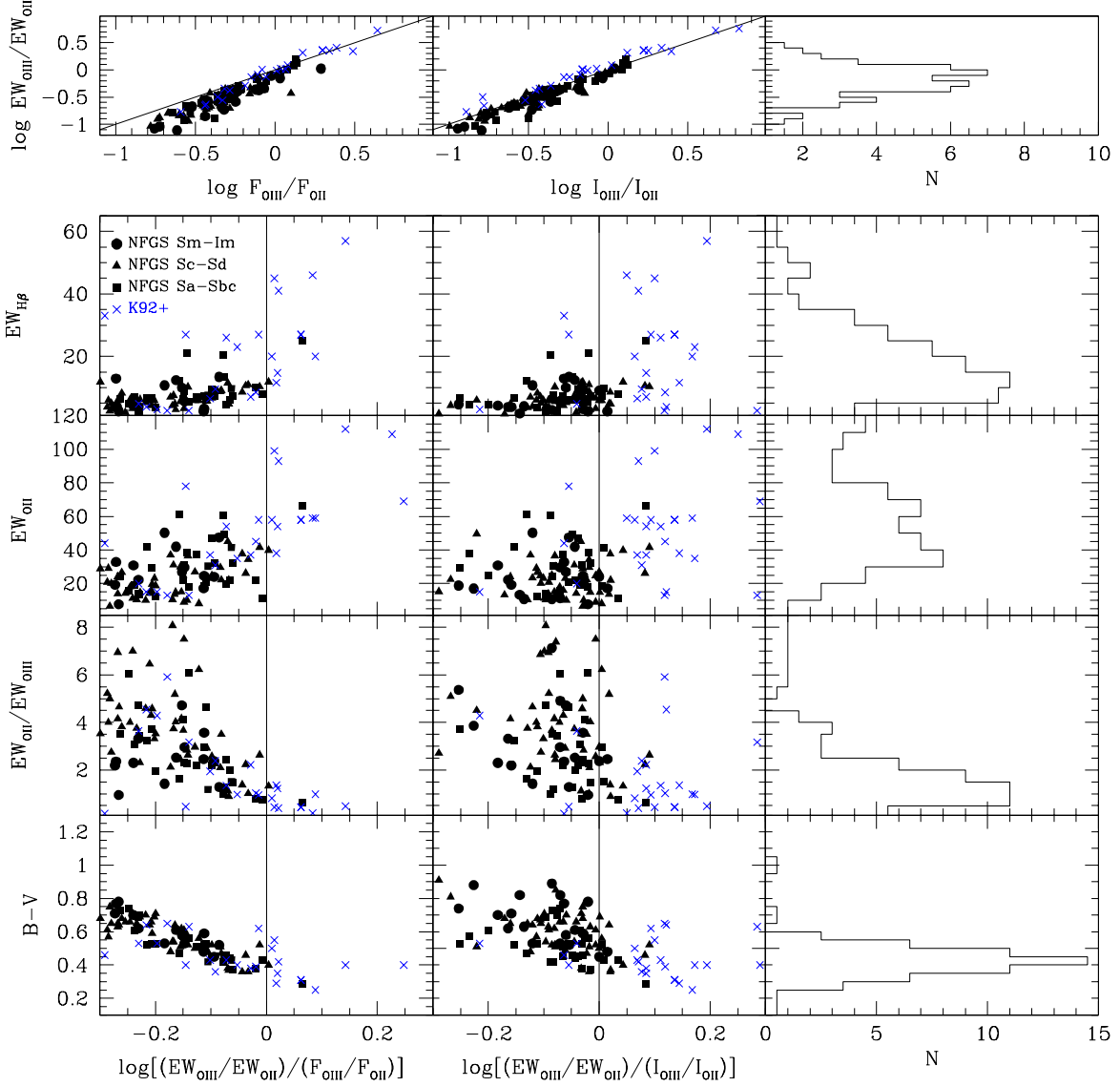


Fig. 6.— Comparison of the ionization parameter quantity $\log(EW_{[\text{O III}]} / EW_{[\text{O II}]})$ with $\log(F_{[\text{O III}]} / F_{[\text{O II}]})$ and the dereddened ratio $\log(I_{[\text{O III}]} / I_{[\text{O II}]})$ for the K92+ and NFGS galaxies. Lower panels show the residuals from the 1-to-1 correspondence as a function of line strength and galaxy color.

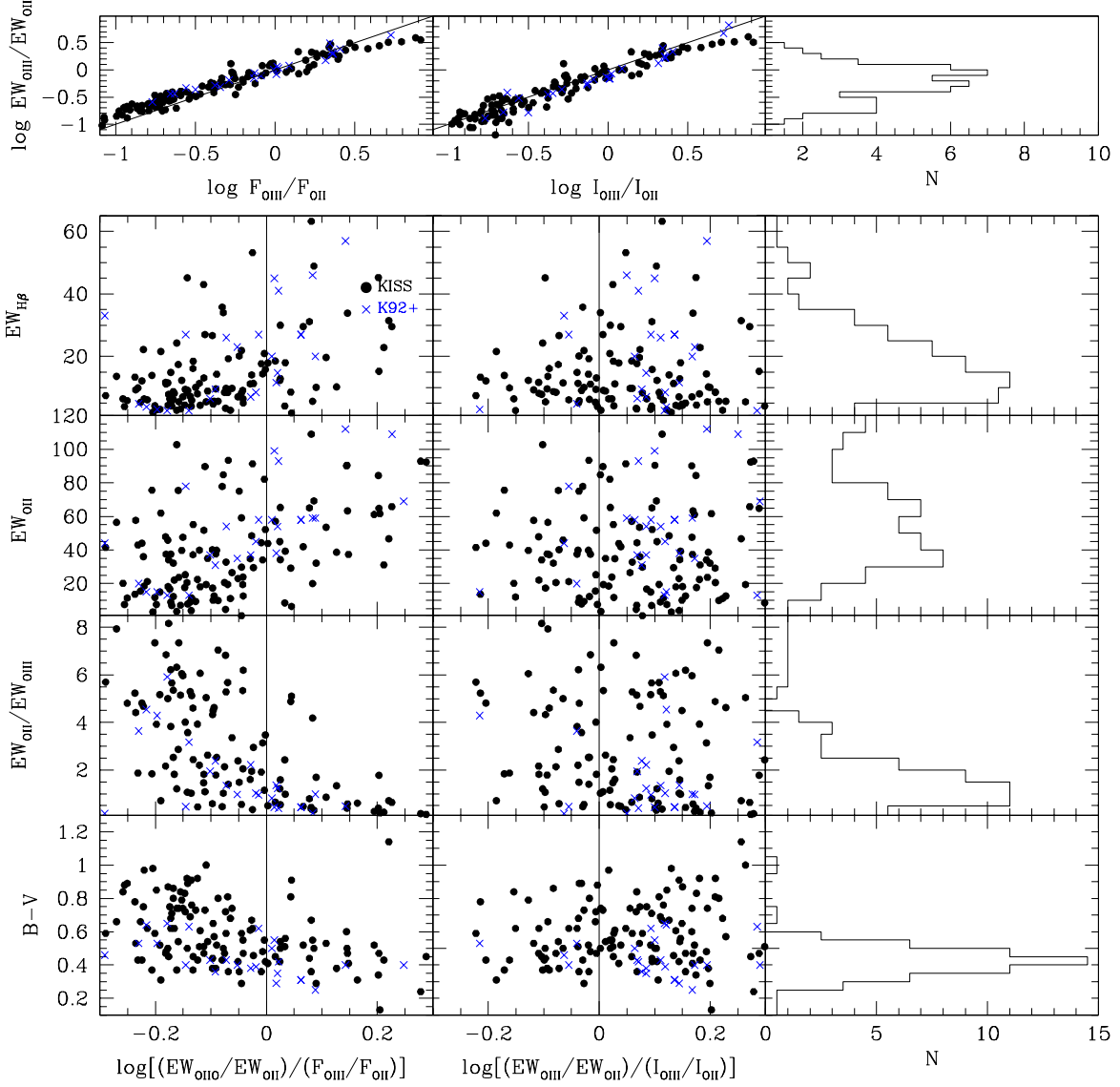


Fig. 7.— Comparison of the ionization parameter quantity $\log(EW_{[O III]}/EW_{[O II]})$ with $\log(F_{[O III]}/F_{[O II]})$ and the dereddened ratio $\log(I_{[O III]}/I_{[O II]})$ for the K92+ and KISS galaxies. Lower panels show the residuals from the 1-to-1 correspondence as a function of line strength and galaxy color.